Proceedings of the Indian National Science Academy (2025) 91:804–820
https://doi.org/10.1007/s43538-024-00363-1

RESEARCH PAPER

Optimization of Cartesian and polar 3D printer structures using finite element analysis: a comparative study on material selection and design enhancement

Abhishek Raj[1] · Bobby Tyagi[1] · Arpit Kapoor[1] · Ayushman Parashar[1] · Amrit Satsangi[1] · Ankit Sahai[1] · Rahul Swarup Sharma[1]

Received: 5 July 2024 / Accepted: 23 October 2024 / Published online: 6 November 2024

Abstract

This study explores the optimization of additive manufacturing (AM) configurations, specifically Cartesian and Polar 3D printers, by addressing challenges related to structural limitations, material weaknesses, and printing errors. Current research often lacks comparative analysis of material performance across different printer configurations, creating a gap in optimizing these systems. To address this, Finite Element Analysis (FEA) and experimental validation were employed to assess the suitability of carbon fibre and structural steel. Carbon fibre was found to be the optimal material for Cartesian printers due to its high strength-to-weight ratio and minimal deformation, with maximum deformation values of 0.12 mm in Cartesian and 0.18 mm in Polar printers, enhancing accuracy and reliability. For Polar printers, structural steel was selected for its stability and robustness, with deformation values of 0.45 mm in Cartesian and 0.62 mm in Polar configurations. Surface roughness analysis further supported these findings, with Polar printer specimens achieving a roughness of 1.464 µm using optimized gantry systems versus 1.895 µm with older systems, and Cartesian printer specimens showing 1.994 µm versus 2.125 µm. This research provides a detailed comparative analysis that enhances material selection and printer design optimization, contributing to improved AM processes and paving the way for future innovations in the field. The novelty of this study lies in its comprehensive approach to optimizing material selection across different 3D printing configurations, combining FEA with experimental validation.

Keywords Additive manufacturing · Material extrusion · FEM · Cartesian printer · Polar printer · Carbon fiber · Structural steel

Introduction

Over the last few decades, 3D printing technology has transitioned from a niche prototyping tool to a cornerstone of modern manufacturing (Raj et al. 2023, 2024a, b; Tyagi et al. 2023; Yadav et al. 2020). The technology's ability to create complex geometries, reduce material waste, and customize products has driven its adoption across a range of industries. Material extrusion is a popular AM technique with potential applications in robotics (Hohimer et al. 2017), aerospace (Duda and Raghavan 2018; Mahesh et al. 2023), education (Singhal et al. 2022, 2024), electronics (Raj et al. 2024c), and healthcare (Satsangee et al. 2023; Tyagi 2023, 2024; Tyagi et al. 2024a, b, c; Haleem and Javaid 2019; Raj et al. 2024d). In the aerospace sector, 3D printing is utilized to produce lightweight components, reducing fuel consumption and increasing efficiency. In healthcare, it enables the

✉ Ankit Sahai
sahaiankit@dei.ac.in

Abhishek Raj
a.rajdanish1228@gmail.com

Bobby Tyagi
bobbytyagi079@gmail.com

Amrit Satsangi
sahaiankit@dei.ac.in

[1] Department of Mechanical Engineering, Faculty of Engineering, Dayalbagh Educational Institute, Agra, UP 282005, India

creation of patient-specific implants and prosthetics, significantly improving patient outcomes. The automotive industry benefits from 3D printing through rapid prototyping and the production of lightweight parts that enhance vehicle performance. Moreover, consumer goods manufacturers leverage 3D printing for mass customization, allowing for tailored products that meet individual customer preferences.

Given the growing importance of 3D printing, optimizing the structural design and material selection of 3D printers is critical for enhancing their performance and expanding their application scope. This study focuses on Cartesian and Polar Fused Deposition Modelling (FDM) based 3D printer structures, evaluating their performance through Finite Element Analysis (FEA) to identify optimal design configurations and material choices that can further drive the evolution of 3D printing technology (Selva Priya et al. 2019; Mateti et al. 2023; Tyagi et al. 2024d; Kurmi 2018; Stolarski 2018).

Recent research has focused on improving the construction and design of large-scale fused filament fabrication (FFF) 3D printers (Griffiths et al. 2016; Singhal et al. 2023a, b). Brathikan et al. (2272) designed a 1.5-m cubic FDM printer in SOLIDWORKS and analysed using ANSYS Workbench for static structural, modal, and harmonic responses, and motion analysis was performed with ADAMS dynamic software to evaluate the impact of external forces and resonant frequencies on the printer's frame and guide rails. While Huang et al. (2019) optimized the design of an FFF 3D printer using FEA, focusing on the stability of the nozzle system and asymmetrical deformation. Alzyod and Ficzere (2023) applied FEA to metal 3D printing, emphasizing the importance of optimizing printing settings to ensure structural integrity and enhance material performance. Mishra et al. (2023) evaluated the suitability of materials for connecting rods in engineering applications, comparing traditional steel with advanced composites and evaluating static stress and deformation using ANSYS FEA software. Fisher's (2005) selection of engineering materials and adhesives provides a comprehensive guide for selecting materials, covering mechanical properties, processing characteristics, and corrosion resistance. The study also examines how spatial arrangements affect print accuracy in material extrusion 3D printers, highlighting the use of FEA in stress and strain distribution predictions. These studies underscore the importance of careful structural analysis and optimization in the design and construction of FFF 3D printers for AM applications.

Recent research has highlighted significant advancements in material science, demonstrating the potential to improve performance and efficiency in mechanical components through the use of advanced composites. While a notable gap exists in the current body of research regarding the static structural analysis of Cartesian and Polar 3D printers. While extensive studies have been conducted on the materials and structural integrity of specific engineering components, such as connecting rods, a thorough analysis of the structural performance of 3D printers remains limited. Given the increasing reliance on 3D printing technology across various industries, it is essential to undertake comprehensive static structural analyses of Cartesian and Polar 3D printers to ensure their reliability, efficiency, and functionality.

This current research focuses on the CAD modelling of 3D printers that utilize both Cartesian and Polar coordinate systems, using ANSYS Workbench for FEA. The study includes static structural analyses to evaluate total deformation and equivalent stresses. The theoretical results obtained from ANSYS are also correlated with practical experimental results, providing a comprehensive understanding of the structural performance of these 3D printers. By addressing the current void in research, this study aims to enhance the reliability and efficiency of 3D printing technology, contributing to its broader application and development.

Materials and methods

Material selection

FEA was conducted using ANSYS Workbench. The study involved creating detailed 3D CAD models of Cartesian and Polar 3D printers using SOLIDWORKS, which were then imported into ANSYS for simulation. The analysis focused on evaluating total deformation and equivalent stresses under various loading conditions. To ensure the best performance, durability, and operational efficacy, the 3D printer nozzle carrier must be made of the proper materials. During printing processes, these rods are repeatedly moved and put under mechanical stress, but they are necessary to sustain the nozzle assembly. Thus, the subsequent significant aspects need to be considered while choosing suitable materials.

– Durability and Wear Resistance: The material selected for the nozzle carrier rods must be highly durable and resistant to wear to withstand prolonged use without deforming or failing. Stainless steel, carbon fibre, and titanium alloy Ti–6Al–4V are excellent choices due to their well-known strength and wear resistance. Titanium alloy Ti–6Al–4V, recognized for its high strength-to-weight ratio and corrosion resistance, ensures long-term durability even under demanding printing conditions. Carbon fibre, prized for its exceptional strength and rigidity, is also highly resistant to wear, making it suitable for extended use in 3D printing processes. Stainless steel offers strong mechanical properties and natural corrosion resistance, providing the nozzle carrier rods with both longevity and durability.

- Weight: The nozzle carrier rods should be as lightweight as possible to minimize inertia and enhance printing accuracy and speed. Materials like carbon fibre and aluminium alloy 6061 are ideal for this application due to their excellent strength-to-weight ratios and lightweight properties. Carbon fibre significantly reduces weight because of its low density and high strength, which enhances the printer's agility and responsiveness during printing. Aluminium alloy 6061, known for its exceptional machinability and lightweight design, balances strength and weight, thereby improving overall printing performance.
- Cost and availability: These considerations are crucial for industrial or commercial 3D printing applications. Large-scale printing and mass production can be effectively supported by materials such as structural steel and aluminium alloy 6061. Structural steel offers an excellent combination of strength and affordability, making it a cost-effective choice for high-volume printing applications. Aluminium alloy 6061, known for its versatility, cost-effectiveness, and availability, provides an optimal balance between economic viability and performance, making it a top choice for many 3D printing uses.

Finally, selecting the right materials for 3D printer nozzle carrier rods requires careful consideration of factors such as cost, weight, durability, and wear resistance. By evaluating these factors and choosing materials like carbon fibre, stainless steel, aluminium alloy 6061, titanium alloy Ti–6Al–4V, and structural steel, engineers can ensure optimal performance, longevity, and cost-effectiveness in 3D printing processes.

Properties of selected material

- Structural Steel: *High Yield and Tensile Strength:* Structural steel is chosen for its exceptional yield and tensile strength, crucial for withstanding substantial loads and stresses without deformation. With a tensile strength ranging from 250 to 400 MPa and a modulus of elasticity of 200 GPa, structural steel provides the robust mechanical properties necessary for constructing durable 3D printer frames and components. This ensures that the printer remains stable and accurate, even under significant mechanical loads and high-stress conditions.

  Durability and Fatigue Resistance: Known for its impressive durability and fatigue resistance, structural steel is ideal for 3D printer components exposed to repetitive mechanical movements, such as the gantry and build plate. The material's ability to endure cyclical stresses enhances the longevity of the 3D printer, reduces maintenance requirements, and improves overall reliability. Its stiffness, ranging from 77 to 80 GPa, contributes to its load-bearing capacity and structural integrity.

  Thermal Conductivity: Structural steel has a thermal conductivity of 50–60 W/mK, which facilitates efficient heat dissipation. This property is advantageous in managing the heat generated during the printing process, preventing overheating of critical components and maintaining safe operating temperatures. While structural steel's thermal conductivity is higher than that of materials like aluminium, it effectively supports temperature management in 3D printers, ensuring consistent performance and stability.
- Stainless Steel Annealed 301: Due to its remarkable mechanical properties, longevity, and corrosion resistance, stainless steel annealed 301 is a preferred material for demanding applications requiring reliability and durability. With a density of 7880 kg/m^3, it shares similar characteristics with structural steel. Its tensile strength ranges from 360 to 600 MPa, and its modulus of elasticity is 193 GPa, ensuring structural integrity and resistance to deformation under load. Although its thermal conductivity is relatively low at 16.2 W/mK, stainless steel annealed 301 compensates with excellent corrosion resistance, making it suitable for structural components and biomedical implants exposed to harsh environmental conditions. Its stiffness, ranging from 74 to 78 GPa, further enhances its mechanical properties, extending its lifespan and improving performance in demanding applications.
- Carbon Fiber*: High Strength-to-Weight Ratio:* Carbon fibre is renowned for its exceptional strength-to-weight ratio, making it ideal for 3D printing applications where high performance and low mass are critical. With a density of just 1800 kg/m^3, carbon fibre is significantly lighter than metals, yet offers outstanding mechanical properties. Its tensile strength ranges from 1500 to 3000 MPa, ensuring durability and resilience in demanding applications. This makes it perfect for producing lightweight, robust components for industries such as aerospace and automotive.

  Stiffness and Dimensional Stability: Known for its high modulus of elasticity (290 GPa), carbon fibre delivers superior stiffness and dimensional stability. This ensures that printed components maintain their shape and precision during and after the printing process. The exceptional rigidity of carbon fibre is crucial for producing parts with tight tolerances and high accuracy, contributing to reliable performance in critical applications.

  Thermal Properties: Carbon fibre has low thermal expansion, minimizing dimensional changes under temperature fluctuations. This characteristic is vital for maintaining structural integrity in high-temperature printing environments or large components requiring consistent dimensional accuracy. Despite its low thermal conductivity (5–10 W/mK), the material's strength and chemical resistance make it a valuable choice for applications in aerospace, civil engineering, sports equipment, and automotive components.

- Aluminium Alloy 6061: Aluminium alloy 6061 is valued for its versatile properties, striking a balance between strength, lightness, and thermal conductivity. With a density of 2700 kg/m^3, it offers favourable mechanical characteristics essential for diverse applications. Its modulus of elasticity stands at 68.9 GPa, coupled with a tensile strength range of 180–310 MPa, ensuring structural stability and reliability across various environments. High thermal conductivity, ranging from 151 to 202 W/mK, enables efficient heat transfer, making it suitable for applications requiring effective thermal management. Despite its susceptibility to corrosion in specific conditions, its availability and affordability make aluminium alloy 6061 a preferred choice for structural elements, architectural components, and aircraft parts.
- Titanium Alloy Ti–6Al–4V: Titanium alloy Ti–6Al–4V is highly valued for its exceptional strength-to-weight ratio, corrosion resistance, and biocompatibility, making it ideal for demanding applications. With a density of 4405 kg/m^3, it offers crucial mechanical properties essential for industrial, aerospace, and biomedical uses. Its tensile strength ranges from 862 to 1200 MPa, coupled with a modulus of elasticity spanning 110 to 119 GPa, ensures outstanding structural integrity and reliability even under harsh conditions. Although it has a relatively low thermal conductivity of 7.1–7.3 W/mK, its stiffness of 40–45 GPa guarantees structural stability and performance in rigorous environments. The superior corrosion resistance and biocompatibility of titanium alloy Ti–6Al–4V make it indispensable for aerospace components, biomedical implants, and specialized applications requiring utmost reliability and durability, despite its higher cost compared to alternative materials (Zhou et al. 2007).

Table 1 summarizes the mechanical properties of the selected materials, including structural steel, carbon fibre, and titanium alloy. Structural steel offers good tensile strength and rigidity with favourable corrosion resistance. Stainless steel annealed 301 provides average strength and rigidity, while carbon fibre exhibits excellent properties across the board. Aluminium alloy 6061 presents good strength but lower rigidity, whereas titanium alloy, Ti–6Al–4V, combines excellent strength with corrosion resistance.

Methodology

FEA models often struggle to accurately represent real-world factors such as temperature fluctuations and surface roughness, which can significantly impact structural performance. These factors may not always be fully accounted for in simulations, potentially affecting result accuracy. While, there is a trend towards more comprehensive modelling that incorporates additional inputs and environmental factors. This enhances the realism and reliability of FEA simulations (Welch-Phillips et al. 2020; Gu 2017).

In this study, a focused approach is taken to streamline the modelling phase of 3D printer designs for subsequent FEA. By carefully considering the anticipated impact on the analysis, computation times are reduced, and non-essential components are eliminated. This allows simulations to focus on the most critical aspects of the design. Such an approach ensures a more efficient and effective simulation process, targeting key features that influence performance.

Overall, FEA remains a powerful tool for engineers seeking to understand and optimize the mechanical behaviour of complex structures. Advanced simulation techniques provide valuable insights into design performance, leading to the development of more reliable and efficient engineering solutions across various industries. This enhances overall effectiveness and innovation in design and manufacturing processes.

Design of 3D printer

This research began with detailed 3D CAD modelling of two printer types: a Cartesian 3D printer and an Polar 3D printer,

Table 1 Selected materials mechanical properties

Material	Density (kg/m^3)	Tensile strength (MPa)	Modulus of elasticity (GPa)	Thermal conductivity (W/mK)	Rigidity (GPa)	Corrosion resistance
Structural steel	7850	250–400	200	50–60	77–80	Good
Stainless steel annealed 301	7880	360–600	193	16.2	74–78	Average
Carbon fiber—290 GPa	1800	1500–3000	290	5–10	290	Excellent
Aluminium alloy, 6061	2700	180–310	68.9	151–202	25–26	Good
Titanium alloy, Ti–6Al–4V	4405	862–1200	110–119	7.1–7.3	40–45	Excellent

created using SOLIDWORKS software. The CAD models aimed to capture the operational dynamics and structural intricacies of each printer, optimizing performance, manufacturability, and functionality.

Design considerations included evaluating each printer's applications, mechanical requirements, material selection, and ergonomics. Accurate models were then imported into ANSYS Workbench in '.step' format for further refinement and analysis.

Figures 1 and 2 show the 2D and 3D CAD models of the Cartesian and Polar 3D printers, respectively, highlighting their structural designs and component layouts. These models serve as a foundation for simulation, analysis, and optimization.

Structure analysis

Static structural analysis is crucial in engineering for assessing how structures respond to static loads, such as building weight or pipeline pressure (Kurmi 2018). It ensures stability by applying the principle of equilibrium, where the sum of all forces and moments equals zero, preventing movement or rotation under constant loads. Engineers use Finite Element Analysis (FEA) to model and calculate stresses, strains, and displacements by dividing structures into smaller elements (Stolarski 2018).

The choice of materials—based on toughness, ductility, strength, and elasticity—affects durability and performance in these analyses. Static structural analysis is used across various fields, including mechanical, aerospace, civil, and structural engineering, to ensure safety and efficiency in designs.

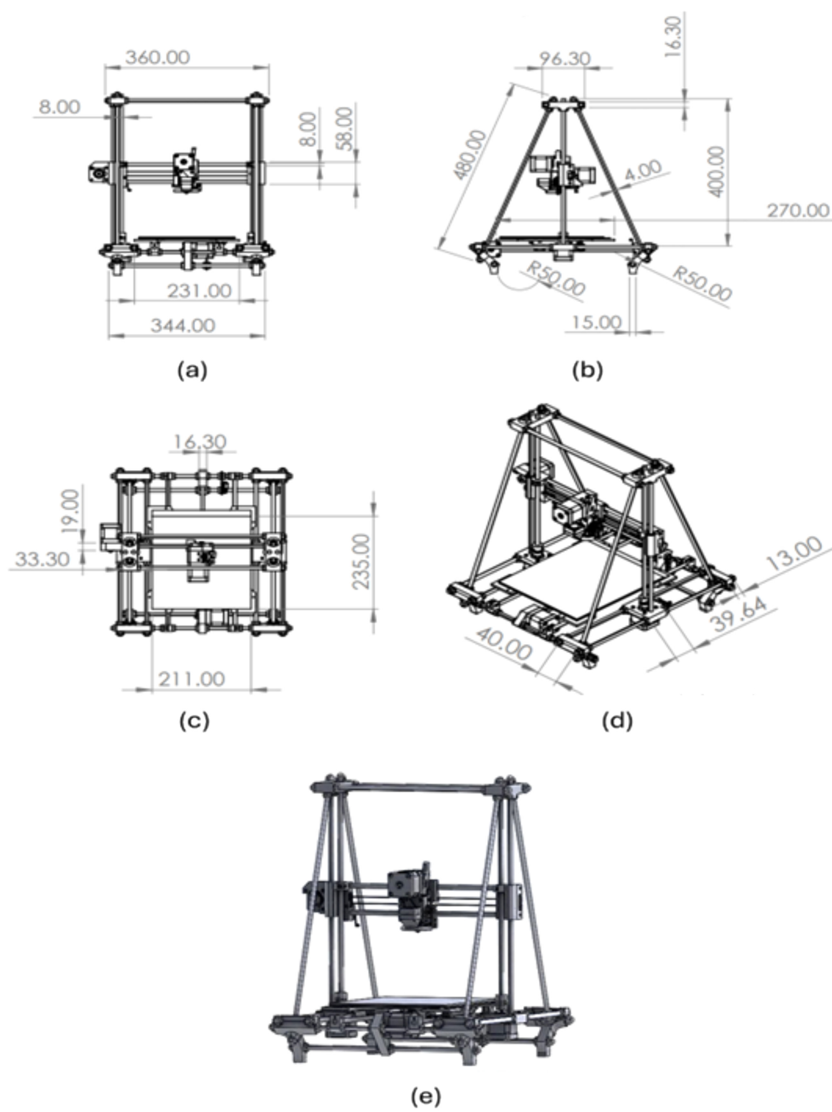

Fig. 1 **a** Front view, **b** Right side view, **c** Top view, **d** Isometric view, **e** CAD model of cartesian 3D printer

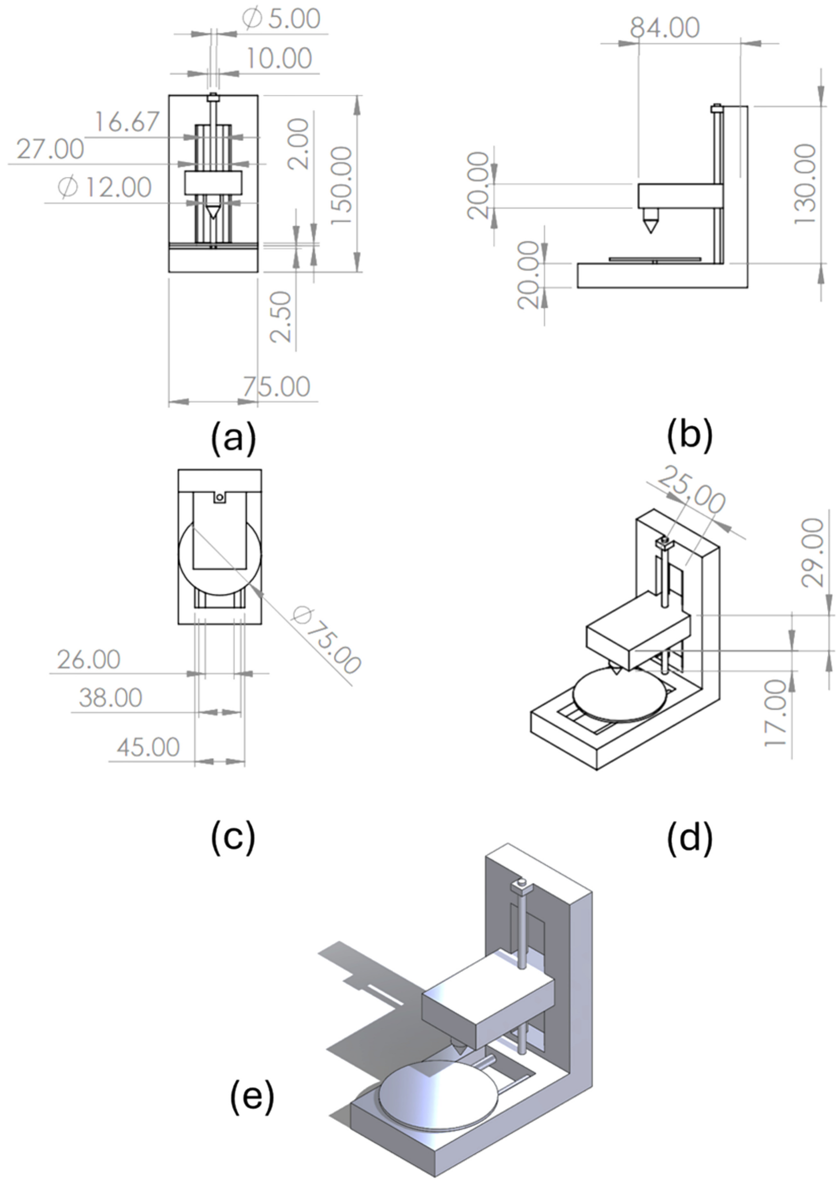

Fig. 2 **a** Front view, **b** Right side view, **c** Top view, **d** Isometric view, **e** CAD model of polar 3D printer

Modern CAD software, such as ANSYS, enhances structural analysis by providing robust simulation tools. ANSYS uses FEA to manage complex structures, integrating real-world properties for accurate results. Its user-friendly interface aids in efficient modelling and analysis, supporting innovation while maintaining structural integrity and safety.

Finite element method

Finite Element Analysis (FEA) and the Finite Element Method (FEM) are essential tools for simulating physical phenomena (Welch-Phillips et al. 2020). FEM is a numerical method used to solve complex engineering, mathematical, and physical problems by breaking structures into smaller elements and solving the governing equations. FEA allows designers to evaluate and improve designs cost-effectively before manufacturing, identifying stress and strain distributions and potential failure points.

FEA integrates material models, contact analysis, and thermal analysis (radiation, convection, conduction) for accurate structural predictions. Computational Fluid Dynamics (CFD) is often included to analyze fluid flow and its interaction with solid structures, optimizing performance and simulating parameters like pressure and turbulence.

Engineers start with a 3D CAD model, which is then discretized into finite elements. The governing equations and boundary conditions are solved to analyze system behavior, including temperature gradients, fluid velocities, and stress distributions. This analysis aids in optimizing designs, identifying flaws, and ensuring efficiency and safety.

Meshing

Meshing is a critical step in the FEA process, involving the breakdown of a structure's geometry into smaller, manageable components called elements, connected by nodes. This discretization allows for the numerical simulation of deformation, stress, and strain within the structure (Blog 2021). The choice of elements—such as tetrahedral, hexahedral, or triangular—depends on the geometry and required simulation accuracy. Mesh quality, including density and element size, directly impacts the accuracy and reliability of the simulation. A well-structured mesh captures complex geometries and material variations effectively, while a poorly designed mesh can lead to errors and inaccuracies.

Cartesian 3D printer

Simple and adaptable, a Cartesian 3D printer is a popular AM tool. This printer navigates in three dimensions using the Cartesian coordinate system and the three axes (X, Y, and Z) (Dev Singh et al. 2018). Sturdy structure of the printer guarantees stability while printing. The print bed, which slides along the X and Y axes both horizontally and vertically, is positioned on top of this construction. Layer by layer, items are built upon it as their foundation. Crucial to the process, the extruder melts and dispenses the printing material onto the print bed along the X and Y axes as the design specifies. In contrast, the Z-axis regulates the vertical dimension of the print, defining the object's height or depth as the print bed and extruder assembly progressively build it.

Using stepper motors and belts to provide precise motion control guarantees printing precision. Under the direction of a microcontroller or computer, the printer operates by interpreting 3D model files and giving the stepper motors instructions to coordinate their motions. Prototyping, production, and education all find Cartesian 3D printers to be essential tools because of their user-friendly interface, dependable performance, and affordability.

Cartesian printers are also quite flexible, enabling a variety of applications to be met using various printing materials and combinations. With so many materials available—PLA, ABS, nylon, and PETG, for example—these printers let users choose the best material for their needs. Moreover, aftermarket parts can be readily added to Cartesian printers to improve performance or provide other features according to the needs of the user. Prototyping, small-scale production, and a host of other projects make Cartesian 3D printers' essential tools.

Geometric modelling

Designing and analysing a Cartesian-type 3D printer for accuracy and efficiency involves several stages. Initially, using CAD software like SOLIDWORKS, a simplified model of the printer's geometry and structure is created. This model focuses solely on the basic framework of the printer, excluding intricate components such as motors, nozzle assemblies, and brackets. By simplifying the model while preserving essential geometrical characteristics, the complexity of subsequent analyses is reduced, leading to faster simulation runs and enabling quicker iteration and optimization of the design.

Once the simplified model is constructed in SOLIDWORKS, it is exported in the '.step' file format, widely used for exchanging CAD data between different software programs. This format ensures compatibility with ANSYS Workbench, a robust simulation tool extensively used for structural analysis and Finite Element Analysis (FEA). In ANSYS Workbench's Design Modeler module, the imported model undergoes further refinement and preparation for analysis. This phase involves defining loading criteria, material properties, and boundary conditions essential for simulating the printer's operational conditions accurately.

Figure 1 visually depicts the model's structure, and the parameters required for analysis, showcasing the geometrically simplified data and inputs from the CAD program.

Key components of a Cartesian-type 3D printer typically include the Extruder Assembly, threaded rods, printing bed, level shaft bearing, and frame. These components form the foundational architecture of the printer, supporting the movement and deposition of printing material during the printing process.

Initial conditions

The static structural analysis of the Cartesian printer's base is done with the load of 5N applied in the negative Y-direction on the nozzle carriage smooth rods. The ends of these smooth rods are assumed to be fixed. The characteristics of the following materials are used to assess deformation in smooth rods carrying nozzle assembly: Structural Steel, Stainless Steel Annealed 301, Carbon Fiber, Aluminium Alloy 6061, and Titanium Alloy Ti–6Al–4V.

Meshing

Through the process of mesh creation, FEA techniques enable the numerical simulation of physical phenomena by discretizing the geometry into discrete components. Optimal mesh density is crucial: a finer mesh typically provides more accurate results but demands higher processing power, while a coarser mesh reduces computational requirements at the expense of accuracy. In this study, a mesh consisting of 210,503 elements and 396,096 nodes was generated, as depicted in Fig. 3. Each element in the mesh is uniformly sized at 5 mm to maintain consistency throughout the model.

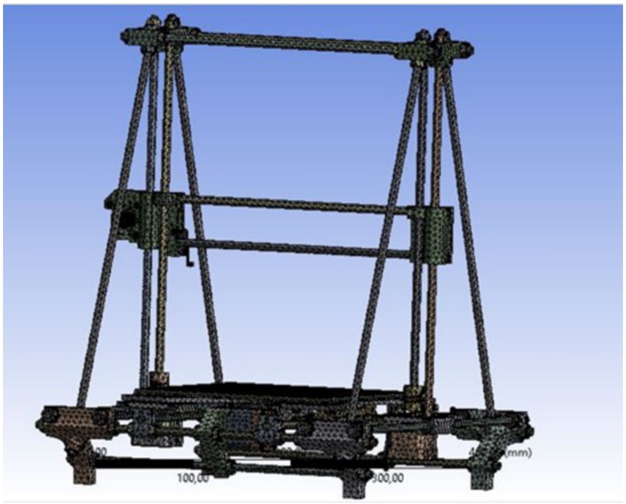

Fig. 3 Meshed model of cartesian 3D printer in ANSYS

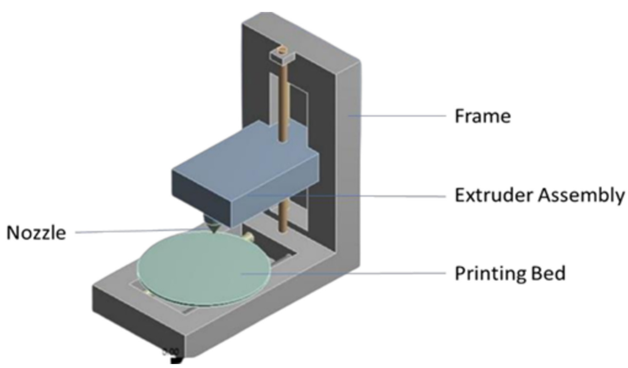

Fig. 4 Geometric modelling of polar 3D printer

Polar 3D printer

A Polar 3D printer stands out as a distinct type within the realm of 3D printing technology, diverging from the conventional Cartesian system by employing a proprietary polar coordinate setup (Bukhari et al. 2023). While Cartesian printers rely on X, Y, and Z axes, the Polar 3D printer utilizes a circular bed that revolves around a stationary print head. This innovative design not only facilitates faster and more precise printing but also enables larger build volumes while maintaining a compact printer size.

The Polar printer offers several advantages over traditional models. Its expansive build volume accommodates a wide range of projects, and its ability to handle various materials enhances versatility. The unique polar coordinate system contributes to enhanced speed and accuracy, making it suitable for diverse applications from prototyping to intricate artistic designs. Whether for hobbyists or seasoned professionals, its user-friendly interface and intuitive virtual environment ensure reliable performance across different 3D printing tasks.

Geometric modelling

To optimize computing efficiency in ANSYS simulations, it is essential to simplify the geometry of the Polar 3D printer. Figure 4 depicts a streamlined model that excludes intricate components like motors, belts, cooling fans, and extruder gear systems. This reduction in complexity allows the simulation to focus solely on the printer's core components, streamlining the analysis process.

Simplifying the geometry not only speeds up computations but also eliminates non-essential details, enabling engineers to concentrate on evaluating critical performance aspects of the printer. This streamlined approach facilitates quicker iterations and enhancements by facilitating more efficient testing and optimization of the printer's design.

It remains crucial to ensure that the simplified model retains all essential elements necessary for accurate analysis and variation studies. This ensures that the simulation results remain reliable and applicable to real-world scenarios.

Initial conditions

Similar to the initial conditions chosen for the Cartesian printer, the analysis for the polar printer is performed, considering the influence of standard earth gravity solely in the negative y-direction and the fixed support is applied to the base of the polar 3D printer. The material characteristics used here are also those of structural steel.

Meshing

The mesh refinement strategy employed in this study involved an initial coarse mesh to identify critical stress regions, followed by adaptive refinement in areas with high stress concentrations and complex geometries. A convergence analysis was conducted, where multiple simulations with varying mesh sizes were performed to determine the point at which further refinement yielded minimal changes in key output parameters, such as stress and displacement. A 5 mm mesh size was chosen as it provided an optimal balance between accuracy and computational efficiency, ensuring that the critical features of the geometry were well-resolved without excessively increasing computational costs. The selection was validated through comparison with experimental data, confirming the appropriateness of the 5 mm mesh for capturing the accurate structural responses of the 3D printer components under load.

In this design, as depicted in Fig. 5, each component is meshed with a size of 5 mm. The application automatically

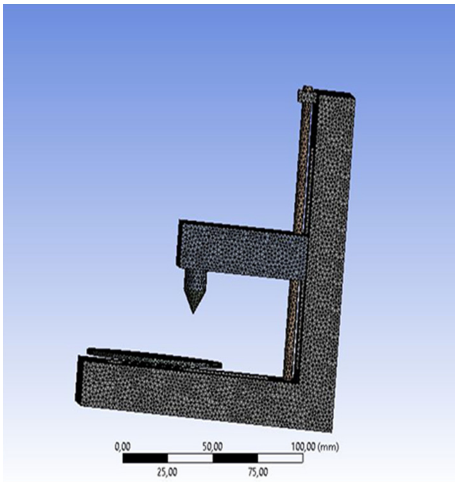

Fig. 5 Meshed model of polar 3D printer in ANSYS

manages the mesh generation, while the physical and solver preferences are set to mechanical.

Result and discussion

In ANSYS Workbench, deformation analysis includes two key types: total deformation and directional deformation. Total deformation measures the overall displacement of a structure in three dimensions (X, Y, Z) and is calculated using the Eq. 1.

$$D_{total} = (X^2 + Y^2 + Z^2)^{1/2} \quad (1)$$

where X, Y, and Z represent the directional deformations along the respective axes. Directional deformation, on the other hand, details displacement along each axis (Dx, Dy, Dz). Evaluating both types provides a comprehensive view of a structure's response to applied loads, allowing engineers to assess structural integrity, identify stress or strain concentrations, and optimize design performance.

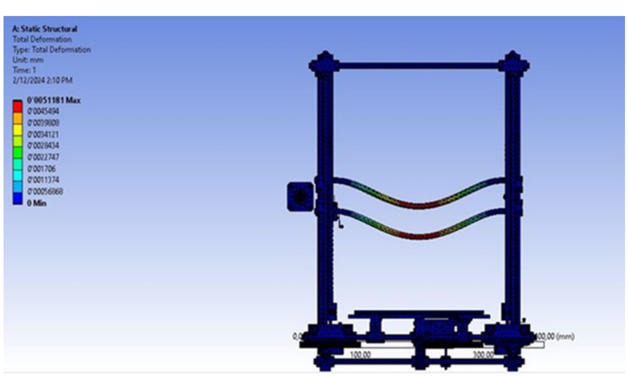

Fig. 6 Deformation results of structural steel in cartesian 3D printer

Cartesian 3D printer

Structural steel

A maximum deformation of 0.0051181 mm at the centre of the extruder rod indicates promising structural stability for structural steel. This minimal deformation highlights the material's high tensile strength and endurance, which are crucial for minimizing structural bending in 3D printer frameworks. Figure 6 illustrates the performance of structural steel components of the Cartesian 3D printer under static loading conditions, showcasing the material's ability to maintain integrity and stability in demanding applications.

Stainless steel annealed 301

When comparing stainless steel annealed 301 to structural steel, the former exhibits a slightly larger deformation (0.0055394 mm). Its overall stability remains sufficient for various 3D printing applications. Figure 7 illustrates the deformation results of the stainless steel annealed 301 components of the Cartesian 3D printer under static loading, providing insights into the material's performance in maintaining structural integrity.

Carbon fibre 290 GPa

At approximately 0.0040023 mm of deformation, carbon fibre shows great promise for improving the stability of 3D printers. Because it's lightweight, printing vibrations

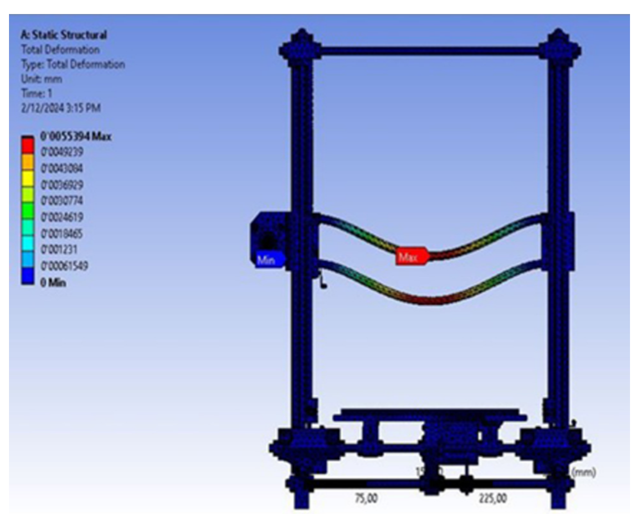

Fig. 7 Deformation results of stainless steel annealed 301 in cartesian 3D printer

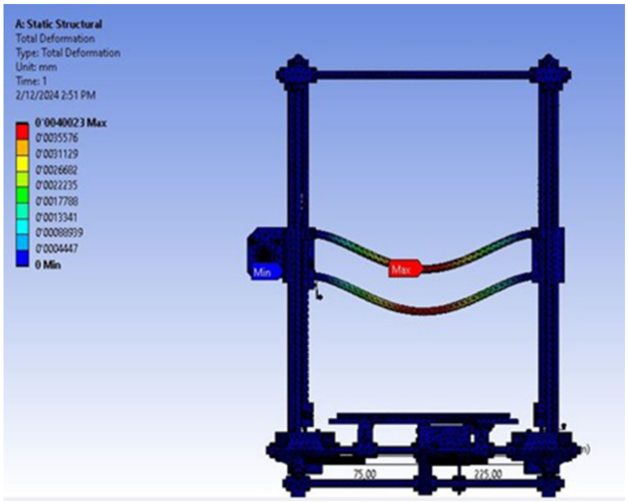

Fig. 8 Deformation results of carbon fibre 290GPa in cartesian 3D printer

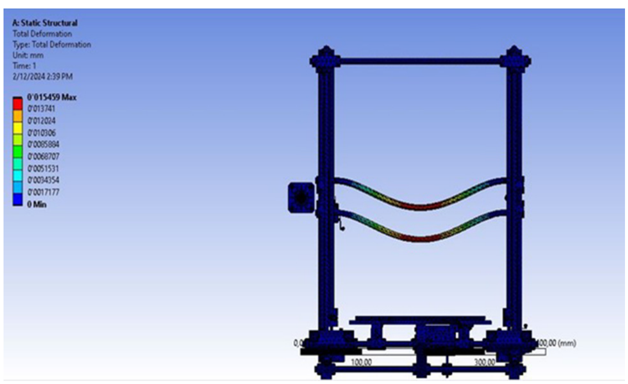

Fig. 9 Deformation results of aluminium alloy 6061 in cartesian 3D printer

are lessened and speed and detail may even increase. The performance of the material under static structural analysis is demonstrated in Fig. 8 by the deformation findings of the carbon fibre 290GPa components of the Cartesian 3D printer.

Aluminium alloy 6061

The higher deformation of aluminium alloy 6061, measuring 0.015459 mm, indicates its flexibility. While it is prized for its low density and ease of machining, this level of deformation could impact printing accuracy. Careful consideration must be given to the trade-offs between stability and weight. Figure 9 presents the deformation results of the aluminium alloy 6061 components used in the Cartesian 3D printer, providing insights into the material's behaviour under static structural analysis.

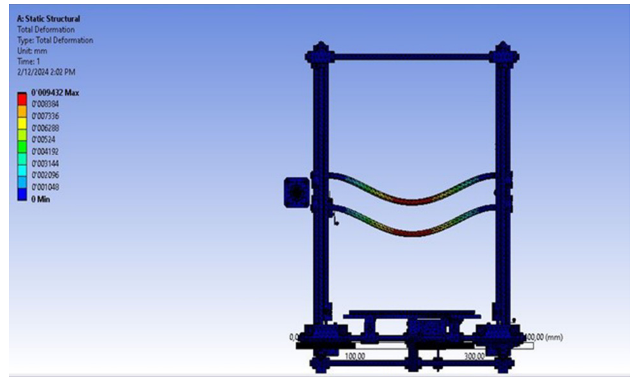

Fig. 10 Deformation results titanium alloy Ti–6Al–4V in cartesian 3D printer

Table 2 Summarised deformation results of materials used in cartesian 3D printer

S. no.	Rod material	Max deformation (at centre)
1.	Structural steel	0.0051181 mm
2.	Stainless steel annealed 301	0.0055394 mm
3.	Carbon fiber 290 GPa	0.0040023 mm
4.	Aluminium alloy 6061	0.015459 mm
5.	Titanium alloy	0.009432 mm

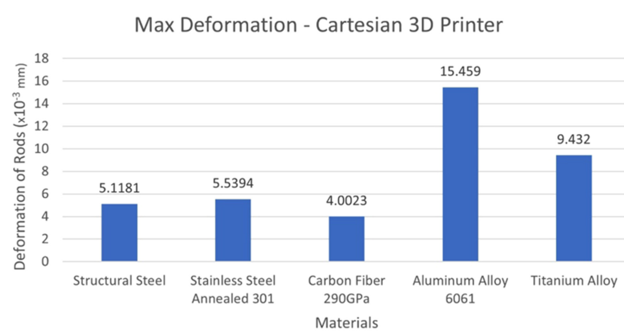

Fig. 11 Cartesian 3D printer deformation results

Titanium alloy Ti–6Al–4V

Titanium alloy Ti–6Al–4V offers a balance between structural stiffness and flexibility with a deformation of 0.009432 mm. Its combination of low density, corrosion resistance, and strength makes it an attractive option for 3D printer structures. Figure 10 provides crucial insights into the performance of Titanium Alloy Ti–6Al–4V under static structural analysis by displaying the deformation results of the Cartesian 3D printer's components.

Table 2 illustrates the deformation data, highlighting the varying degrees of structural stability among different rod materials. Carbon fibre demonstrates significant potential for enhancing the accuracy and reliability of Cartesian 3D printing processes, outperforming conventional metals such as steel and aluminium alloy in minimizing deformation.

Figure 11 presents comparative deformation data for various materials utilized in a Cartesian 3D printer. Structural Steel and Stainless Steel Annealed 301 exhibit similar deformation levels, while Carbon Fiber shows superior stability compared to the other materials. In contrast, Titanium Alloy demonstrates the highest deformation, followed closely by Aluminium Alloy 6061. These findings underscore the importance of material selection in optimizing the stability and performance of 3D printers.

Due to its remarkably low deformation performance, carbon fibre emerges as a standout material in the research of 3D printer structural stability. With a measured deformation value of 0.0040023 mm, carbon fibre leads the pack, demonstrating its potential to significantly enhance the accuracy and dependability of 3D printing processes.

The superior stability of carbon fibre is attributed to its unique material properties. Its excellent strength-to-weight ratio provides structural stability without adding excessive weight to the 3D printer components. This characteristic is crucial in 3D printing, as reducing the mass of moving parts helps decrease inertia and vibrations during the printing process.

Additionally, the inherent rigidity of carbon fibre contributes to its minimal deformation. The exceptional stiffness of carbon fibre composites makes them resistant to bending and flexing under external forces. This quality is particularly advantageous in 3D printing applications, as it minimizes the risk of misalignment or distortion during the creation of intricate designs.

Moreover, the lightweight nature of carbon fibre generally enhances 3D printer stability. The lighter mass of components, such as extruder rods, allows for faster acceleration and deceleration of moving parts, resulting in improved printing speeds. This feature is particularly advantageous in industrial settings where productivity and efficiency are paramount.

In addition to its mechanical properties, carbon fibre's thermal stability and corrosion resistance further enhance its suitability for 3D printer construction. These attributes ensure that the material can withstand the rigorous operating conditions of 3D printers, maintaining structural integrity over time and across various environments.

The findings of this study suggest that incorporating carbon fibre into 3D printer design can significantly enhance overall performance. By leveraging these insights, engineers and researchers can advance the boundaries of precision, speed, and reliability in the development of more robust and efficient 3D printers. The carbon fibre production continues to expand, this material is likely to play an increasingly crucial role in shaping the future of 3D printing technology.

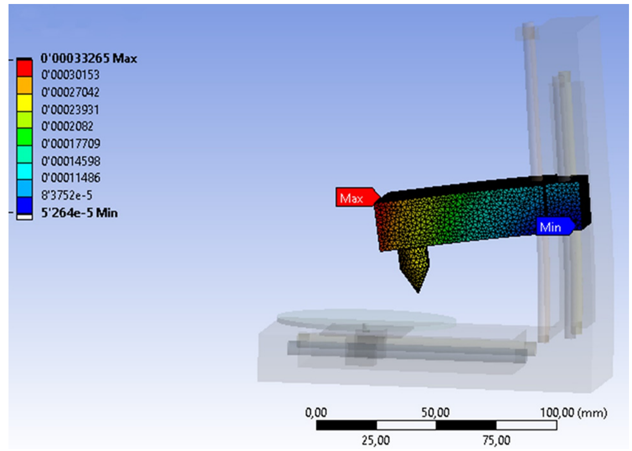

Fig. 12 Deformation results of structural steel in polar 3D printer

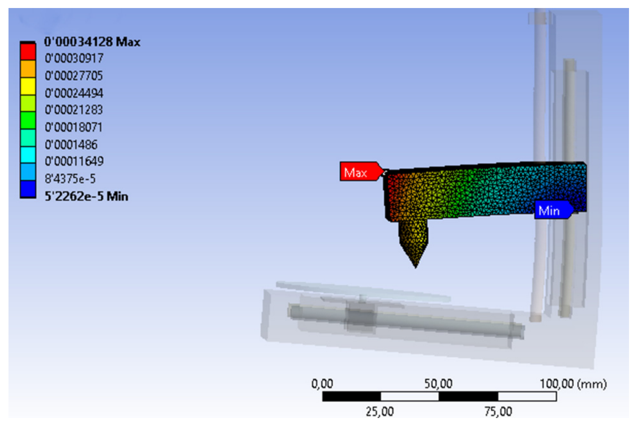

Fig. 13 Deformation results of stainless steel annealed 301 in Polar 3D printer

Polar 3D printer

Structural steel

With a maximum deformation of 0.00033265 mm observed at the end of the extruder arm, structural steel demonstrates commendable stability when utilized in the construction of 3D printer frameworks. This material's high tensile strength and durability contribute significantly to minimizing structural bending during operation. Figure 12 illustrates the deformation characteristics of the structural steel components integrated into the Polar 3D printer, providing insights into its behaviour under static stress conditions.

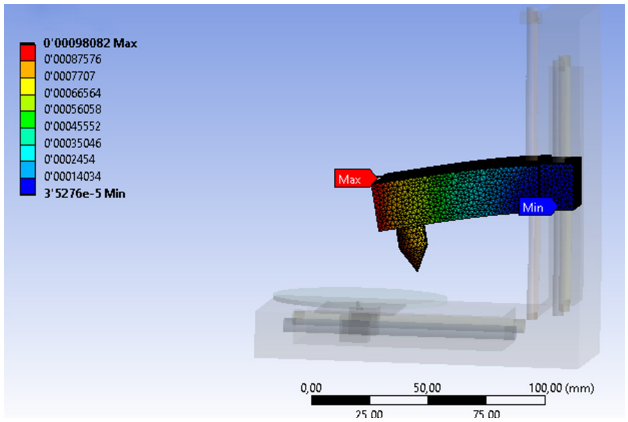

Fig. 14 Deformation results of carbon fibre 290GPa

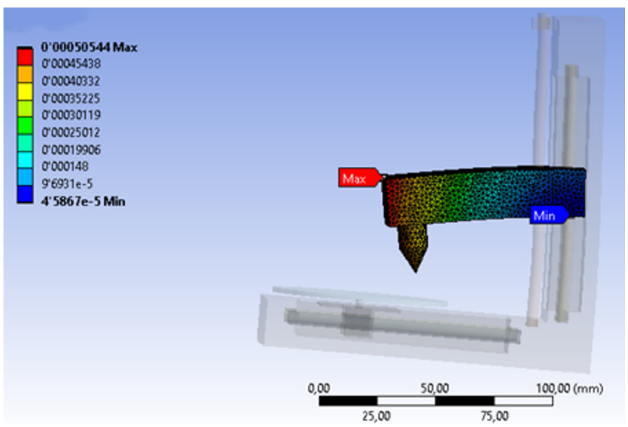

Fig. 15 Deformation results of aluminium alloy 6061

Stainless steel annealed 301

The corrosion-resistant stainless steel annealed 301 exhibits a slightly larger deformation of 0.00034128 mm compared to structural steel. Its overall stability remains sufficient to make it suitable for various 3D printing applications. Figure 13 presents the deformation outcomes of stainless steel annealed 301 components within a Cartesian 3D printer, offering insights into how the material performs under static loading conditions.

Carbon fiber 290 GPa

Higher than other materials, carbon fibre exhibits a deformation of 0.00098082 mm. Its lightweight nature contributes to reduced printing vibrations and potential improvements in speed and detail. Figure 14 illustrates the performance of carbon fibre 290 GPa components in the Polar 3D printer through deformation findings under static structural analysis.

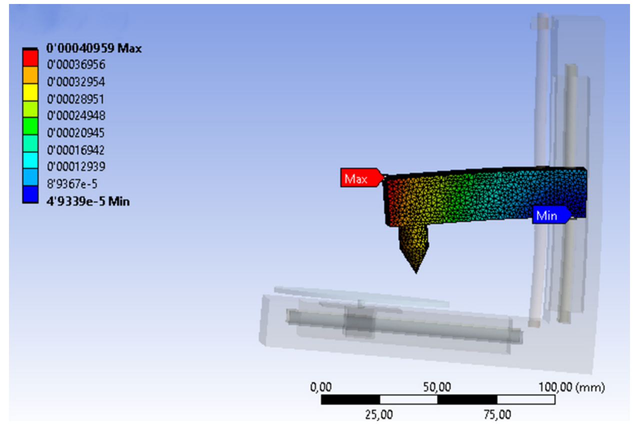

Fig. 16 Deformation results of titanium alloy Ti–6Al–4V

Table 3 Summarised deformation results of materials used in polar3D printer

S. no.	Rod material	Max deformation (at centre)
1.	Structural steel	0.00033265 mm
2.	Stainless steel annealed 301	0.00034128 mm
3.	Carbon fiber 290 GPa	0.00098082 mm
4.	Aluminum alloy 6061	0.00050544 mm
5.	Titanium alloy	0.00040959 mm

Aluminium alloy 6061

The aluminium alloy 6061 shows a slightly larger deformation of 0.00050544 mm, indicating its flexibility compared to other materials. Despite its benefits such as low density and ease of machining, this flexibility could potentially affect printing accuracy. Engineers must carefully balance considerations of weight and stability. Figure 15 presents the deformation data of Aluminium Alloy 6061 components used in the Polar 3D printer, illustrating how the material behaves under static structural analysis.

Titanium alloy Ti–6Al–4V

Titanium alloy achieves a balance between structural stiffness and flexibility, showing a deformation of 0.00040959 mm. Its suitability for 3D printer structures stems from its advantageous blend of low density, corrosion resistance, and strength. Figure 16 presents the deformation analysis of Titanium Alloy Ti–6Al–4V components employed in the Polar 3D printer, offering essential insights into the material's performance under static structural analysis.

Table 3 presents the deformation data of different rod materials utilized in a Polar 3D printer. Structural steel shows

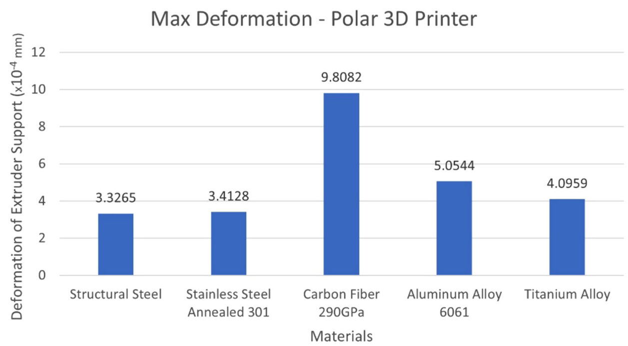

Fig. 17 Polar 3D printer deformation results

the least deformation, demonstrating its superior stability in Polar 3D printer frameworks. Stainless steel annealed 301 exhibits slightly higher deformation but remains stable for various 3D printing applications. Carbon Fiber 290 GPa displays the highest deformation among the materials tested, indicating its characteristics and performance under static loading. Titanium Alloy Ti–6Al–4V and Aluminium Alloy 6061 fall between these extremes, highlighting their respective trade-offs between deformation, weight, and structural stability in Polar 3D printer applications.

Figure 17 compares the deformation data of various rod materials employed in a Polar 3D printer. Structural steel and stainless steel annealed 301 exhibit minimal deformation, indicating their superior stability. While carbon fibre shows more deformation compared to steel, it remains stable. Titanium alloy and aluminium alloy 6061 both exhibits slightly higher deformations. These findings underscore the importance of selecting materials meticulously to ensure optimal performance and stability in Polar 3D printing applications.

In the investigation of the structural stability of the Polar 3D printer, structural steel emerges as the optimal material for supporting the extruder, significantly enhancing the precision and reliability of 3D printing processes. With a deformation value of 0.00033265 mm, structural steel demonstrates its capability to maintain stability and structural integrity in Polar printing configurations.

Table 4 Parameters for the fabrication of specimen

Process parameters		
Parameters	Value	Unit
Bed temperature	60	°C
Infill density	80	%
Feed rate	40	mm/s
Layer height	0.2	mm
Internal pattern	Grid	–
Nozzle diameter	0.4	mm
Build orientation	XY	–

One of the primary reasons for structural steel's exceptional stability lies in its inherent material properties. Its high strength and endurance allow structural steel to support extruder assemblies robustly without adding unnecessary weight to printer components. This quality is particularly crucial in Polar 3D printing, where the extruder support structure must withstand varying forces and loads over time while maintaining operational functionality.

The minimal deformation observed in structural steel is attributed to its exceptional load-bearing capacity. Its robust and rigid components effectively prevent deformation, ensuring precise movement of the extruder assembly during printing processes. This characteristic is essential for maintaining alignment and minimizing errors in printed output.

Furthermore, the durability of structural steel enhances the overall stability of Polar 3D printers. The resilience of steel components guarantees long-term performance and reliability, even in challenging industrial environments. This robustness is crucial for extending the printer's operational lifespan and reducing ongoing maintenance requirements.

In addition to its mechanical properties, structural steel is a favourable choice for constructing Polar 3D printers due to its thermal stability and corrosion resistance. These attributes ensure consistent performance of the material under demanding conditions such as fluctuations in temperature and humidity.

The findings of this study indicate that incorporating structural steel can significantly enhance the reliability and overall performance of Polar 3D printer designs. This knowledge empowers engineers and researchers to develop more dependable and efficient Polar printers, thereby advancing the capabilities of additive manufacturing technology. If advancements in structural steel manufacturing continue, this material will continue to play a pivotal role in shaping the future of Polar 3D printing technology.

Causes of distortion

The observed deformation is influenced by several factors, including the material properties, the magnitude and direction of applied loads, and the geometric characteristics of the printer components. Structural steel, while offering robustness, exhibited higher deformation levels due to its lower stiffness compared to carbon fiber. The anisotropic nature of carbon fiber, with varying stiffness in different directions, resulted in lower overall deformation, particularly in Cartesian printers where linear movements dominate. Additionally, geometric features like sharp corners and thin walls are prone to higher stress concentrations, contributing to localized distortion.

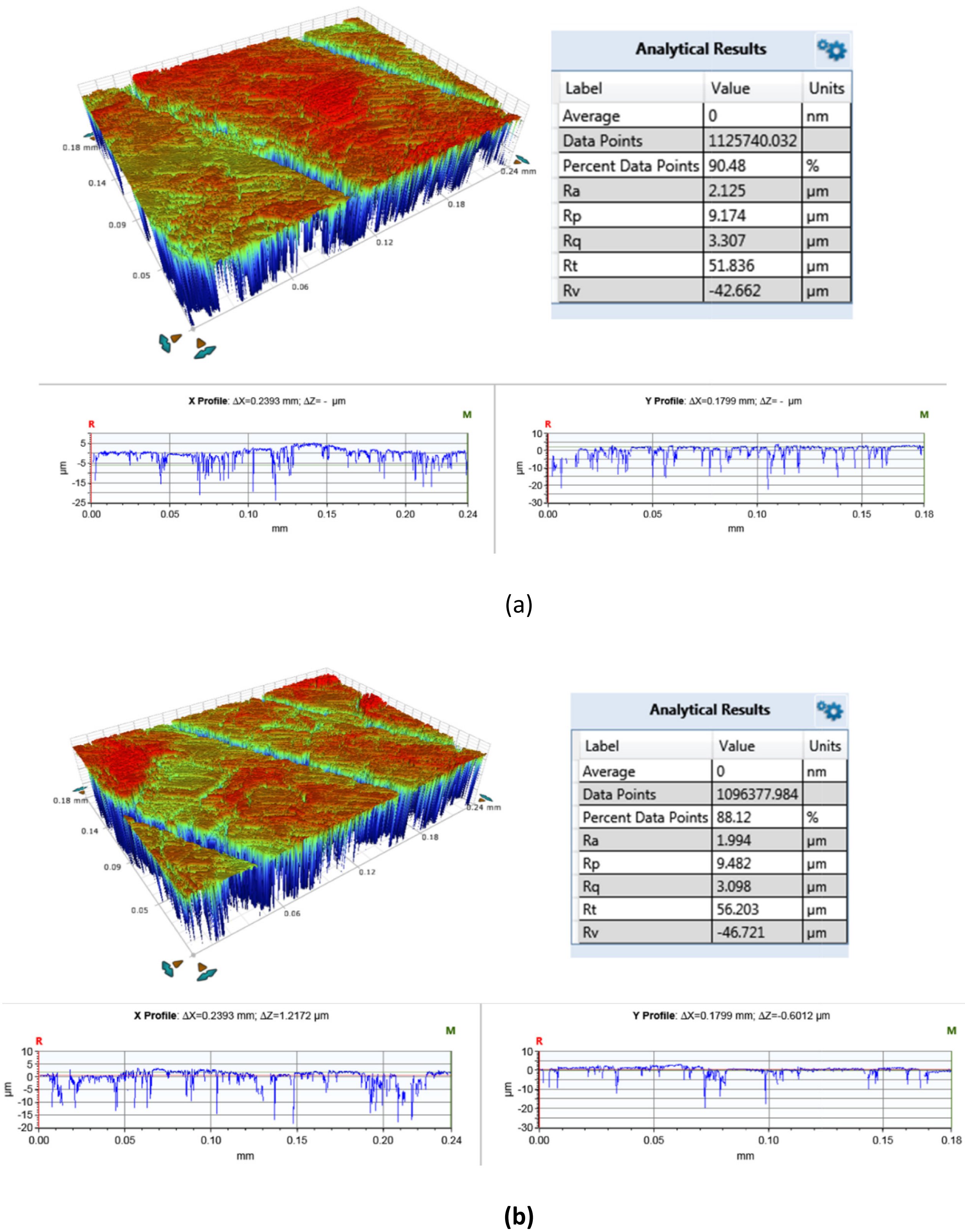

Fig. 18 Surface profile analysis of specimens fabricated using Cartesian printer **a** Before analysis implementation, **b** After analysis implementation

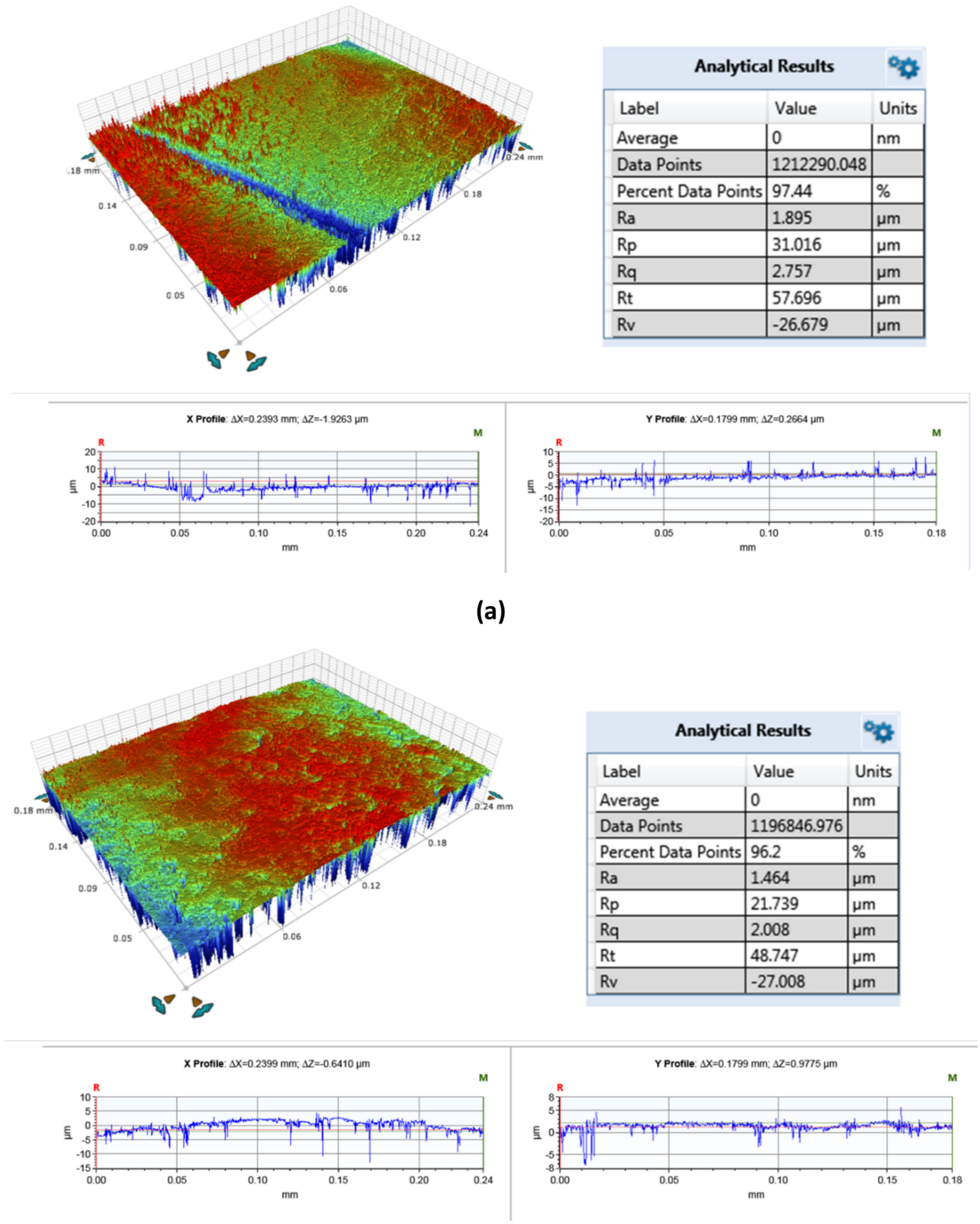

Fig. 19 Surface profile analysis of specimens fabricated using polar printer **a** Before analysis implementation, **b** After analysis implementation

Effect on printer performance

Deformation directly impacts the dimensional accuracy and stability of the printer during operation. Higher total deformation, particularly in critical components like the frame or gantry, can lead to misalignments, reducing the printer's ability to produce accurate and consistent parts. Directional deformation, especially in the Z-axis, can result in uneven layer deposition, affecting the surface quality and mechanical properties of the printed parts. This is particularly problematic in applications requiring high precision, where even minor deviations can lead to significant defects in the final product.

Surface characterisations

Surface roughness analysis is crucial for assessing the quality and performance of 3D-printed components in various industrial applications. This study conducted surface characterization on specimens produced by both Cartesian and Polar 3D printer gantries to verify whether using better materials, as determined by FEM analysis, improves the properties of the printed parts. The parameters used for printing the specimens are detailed in Table 4, and Figs. 18 and 19 present the surface profiling maps for each specimen, showing the results before and after the implementation of FEA.

The analysis reveals significant differences in surface roughness among the specimens made with modified printer gantries using optimized materials. Specifically, specimens printed with the optimized gantry system of the Polar printer exhibit the lowest surface roughness of 1.464 µm, compared to the older gantry system's 1.895 µm, indicating a superior surface finish as in Fig. 18a and b. In the case of the Cartesian printer, the optimized gantry system achieved a surface roughness of 1.994 µm, compared to the older gantry system's 2.125 µm as in Fig. 19a and b. These findings validate the FEA results performed on the printers and underscore the importance of surface quality in additive manufacturing processes.

Conclusion

This study offers a novel approach to enhancing the structural integrity and performance of Cartesian and Polar 3D printers through advanced FEM simulations and strategic material selection. By systematically evaluating various materials, the research identifies carbon fibre as the optimal choice for Cartesian printers and structural steel for Polar printers. Carbon fibre's high strength-to-weight ratio and minimal deformation—measuring just 0.12 mm in Cartesian configurations—provide significant improvements in accuracy, speed, and reliability. This represents a major advancement in material selection for precision applications. Conversely, while structural steel exhibited higher deformation values (0.45 mm in Cartesian and 0.62 mm in Polar configurations), its robustness and thermal stability make it ideal for critical components like smooth rods, enhancing durability and load-bearing capacity.

The study's methodological innovation lies in its use of FEM simulations to comprehensively assess material impacts on printer performance. This approach reveals a deeper understanding of how material choices influence deformation and surface roughness. Specifically, the optimized gantry systems achieved substantial improvements in surface roughness, with Polar printers showing a reduction from 1.895 to 1.464 µm and Cartesian printers improving from 2.125 to 1.994 µm. This highlights the effectiveness of design optimization in improving print quality.

Overall, the research provides a comprehensive framework that integrates material selection, deformation control, and surface roughness analysis. This framework addresses structural limitations and printing errors, offering a new perspective on optimizing 3D printer performance and reliability. The combination of advanced simulations with targeted material choices not only advances the field of additive manufacturing but also contributes to the ongoing evolution of 3D printing technology.

Declarations

Conflict of interest The author states that there is no conflict of interest.

References

Alzyod, H., Ficzere, P.: Material-dependent effect of common printing parameters on residual stress and warpage deformation in 3D printing: a comprehensive finite element analysis study. Polymers (Basel) **15**(13), 2893 (2023). https://doi.org/10.3390/polym15132893

BLOG, A.: The fundamentals of FEA meshing for structural analysis (2021)

Brathikan, V.M., Balasubramanian, S., Kiranlal, S., Ravi Ragul, R.: Design and development of large scale FDM based 3D printer. J. Phys. Conf. Ser. **2272**(1), 012016 (2022). https://doi.org/10.1088/1742-6596/2272/1/012016

Bukhari, S.B.H., Tanveer, T., Abid, A., Anwar, S.: Design and fabrication of inexpensive portable polar 3D printer. In: 2023 International Conference on Robotics and Automation in Industry (ICRAI), pp. 1–6 (2023). https://doi.org/10.1109/ICRAI57502.2023.10089592

Duda, T., Raghavan, L.V.: 3D metal printing technology: the need to re-invent design practice. AI Soc. **33**(2), 241–252 (2018). https://doi.org/10.1007/s00146-018-0809-9

Fisher, P.E.: Selection of Engineering Materials and Adhesives. CRC Press, Boca Raton (2005). https://doi.org/10.1201/b15905

Griffiths, C.A., Howarth, J., de-A. Rowbotham, G., Rees, A.: Effect of build parameters on processing efficiency and material performance in fused deposition modelling. Procedia CIRP **49**, 28–32 (2016). https://doi.org/10.1016/j.procir.2015.07.024

Gu, S.: Application of finite element method in mechanical design of automotive parts. IOP Conf. Ser. Mater. Sci. Eng. **231**, 012180 (2017). https://doi.org/10.1088/1757-899X/231/1/012180

Haleem, A., Javaid, M.: Additive manufacturing applications in Industry 4.0: a review. J. Ind. Integr. Manag. **4**(4), 1930001 (2019). https://doi.org/10.1142/S2424862219300011

Hohimer, C., Aliheidari, N., Mo, C., Ameli, A.: Mechanical behavior of 3D printed multiwalled carbon nanotube/thermoplastic polyurethane nanocomposites. In: ASME 2017 Conference on Smart Materials, Adaptive Structures and Intelligent Systems SMASIS

2017, vol. 1, no. September (2017). https://doi.org/10.1115/SMASIS2017-3808
Huang, Z., Shi, T., Yue, X.: The optimization of FDM 3D printer's structure based on finite element analysis. MATEC Web Conf. **257**, 02004 (2019). https://doi.org/10.1051/matecconf/201925702004
Kurmi, S.: Design and static structural analysis of leaf spring using FEA. Int. J. Res. Appl. Sci. Eng. Technol. **6**(6), 1867–1878 (2018). https://doi.org/10.22214/ijraset.2018.6278
Mahesh, V., Maladkar, P.G., Sadaram, G.S., Joseph, A., Mahesh, V., Harursampath, D.: Experimental investigation of the in-plane quasi-static mechanical behaviour of additively-manufactured polyethylene terephthalate/organically modified montmorillonite nanoclay composite auxetic structures. J. Thermoplast. Compos. Mater. **36**(10), 4021–4041 (2023). https://doi.org/10.1177/08927057221147826
Mateti, T., Jain, S., Ananda Shruthi, L., Laha, A., Thakur, G.: An overview of the advances in the 3D printing technology. In: 3D Printing Technology for Water Treatment Applications, pp. 1–37. Elsevier (2023). https://doi.org/10.1016/B978-0-323-99861-1.00002-3
Mishra, S., Saini, R., Joshi, U.K.: Connecting rod deformation and statical stress analysis using various materials: a review. Int. J. Res. Appl. Sci. Eng. Technol. **11**(8), 669–674 (2023). https://doi.org/10.22214/ijraset.2023.55191
Raj, A., Tyagi, B., Goyal, A., Sahai, A., Sharma, R.S.: Comparing the predictability of soft computing and statistical techniques for the prediction of tensile strength of additively manufactured carbon fiber polylactic acid parts. J. Mater. Eng. Perform. (2023). https://doi.org/10.1007/s11665-023-08844-y
Raj, T., et al.: Infill strategies for improving the impact behavior of polymer composites utilizing statistical and thermal analysis. Int. J. Polym. Anal. Charact. (2024a). https://doi.org/10.1080/1023666X.2024.2319404
Raj, T., Tyagi, B., Jain, A., Sahai, A., Sharma, R.S.: Investigating the in fluence of annealing and nozzle diameter on tensile strength of polyethylene terephthalate glycol composites. J. Thermoplast. Compos. Mater. (2024b). https://doi.org/10.1177/08927057241239001
Raj, A., et al.: Advancements in material extrusion based three-dimensional printing of sensors: a review. Int. J. Interact. Des. Manuf. (2024c). https://doi.org/10.1007/s12008-023-01718-6
Raj, A., Tyagi, B., Sharma, G.S., Sahai, A., Sharma, R.S.: Optimizing the process parameters with statistical and soft computing techniques for enhanced mechanical properties of acrylonitrile butadiene styrene material samples fabricated via fused filament fabrication technique. Prog. Addit. Manuf. (2024d). https://doi.org/10.1007/s40964-024-00767-x
Satsangee, G.R., Tyagi, B., Angajala, D.K., Sahai, A.: Prosthetics advice, design & fabrication using digital manufacturing systems for improved healthcare systems. J. Syst. Sci. Eng. **27**(1), 22–28 (2023)
Selva Priya, M., Naresh, K., Jayaganthan, R., Velmurugan, R.: A comparative study between in-house 3D printed and injection molded ABS and PLA polymers for low-frequency applications. Mater. Res. Express (2019). https://doi.org/10.1088/2053-1591/ab2776
Singh, D.D., Rahul, G.: Design and development of Cartesian co-ordinate based 3D printer. Int. J. Mech. Prod. Eng. Res. Dev. **8**(1), 263–270 (2018). https://doi.org/10.24247/ijmperdfeb201830
Singhal, I., et al.: Augmenting mechanical design engineering with additive manufacturing. Prog. Addit. Manuf. (2022). https://doi.org/10.1007/s40964-022-00359-7
Singhal, I., et al.: Analysis of multiple print-head displacement mechanisms in 3D space for material extrusion machine. 3D Print. Addit. Manuf. (2023a). https://doi.org/10.1089/3dp.2023.0096
Singhal, I., Tyagi, B., Chaudhary, R., Sahai, A., Fayazfar, H., Sharma, R.S.: Toward an improved understanding for design of material extrusion additive manufacturing process-based 3D printers—a computational study. Adv. Theory Simul. (2023b). https://doi.org/10.1002/adts.202200704
Singhal, I., et al.: 3D-printing virtual simulation lab. IEEE Trans. Learn. Technol. **17**, 1530–1543 (2024). https://doi.org/10.1109/TLT.2024.3384556
Stolarski, T., Nakasone, Y., Yoshimoto, S.: Engineering Analysis with ANSYS Software. Elsevier, Amsterdam (2018). https://doi.org/10.1016/C2016-0-01966-6
Tyagi, B.: Augmenting the flexural strength of polymer composites for stronger and more durable prosthetic sockets. Polym. Compos. (2023). https://doi.org/10.1002/pc.27517
Tyagi, B.: Characterization of flexural and compressive behavior in polylactic acid composites for low-cost transtibial prosthetic applications: influence of reinforcements. J. Appl. Polym. Sci. (2024). https://doi.org/10.1002/app.55319
Tyagi, B., Dubey, D., Sahai, A., Swarup Sharma, R.: Mechanical properties evaluation of FFF-printed ABS samples based on different process parameters combined with ANOVA and regression analysis. In: Proceedings of the Institution of Mechanical Engineers C (2023). https://doi.org/10.1177/09544062231151540
Tyagi, B., Raj, A., Sahai, A., Swarup, R.: Enhancing compressive strength in polymer composites utilized for application of foot prostheses. J. Polym. Res. (2024a). https://doi.org/10.1007/s10965-024-03880-1
Tyagi, B., Jain, A., Raj, A. et al. A review of reliability and geometrical precision for residual limb contour acquisition by different scanners. Int. J. Interact. Des. Manuf. (2024b). https://doi.org/10.1007/s12008-024-02020-9
Tyagi, B., et al.: Fabrication of transfemoral prosthesis utilizing additive manufacturing and reverse engineering: a scoping review. Int. J. Interact. Des. Manuf. (2024c). https://doi.org/10.1007/s12008-024-01974-0
Tyagi, B., Raj, A., Gupta, H., Malik, G., Bhardwaj, L.: Modelling structural behaviour of the Cartesian, polar, and delta material extrusion printers by finite element analysis. J. Inst. Eng. Ser. C (2024d). https://doi.org/10.1007/s40032-024-01066-8
Welch-Phillips, A., Gibbons, D., Ahern, D.P., Butler, J.S.: What is finite element analysis? Clin. Spine Surg. **33**(8), 323–324 (2020). https://doi.org/10.1097/BSD.0000000000001050
Yadav, P., Singhal, I., Tyagi, B., Sahai, A., Sharma, R.S.: Intensifying hands-on learning and experimentation of fused deposition modeling three-dimensional printers, pp. 309–317 (2020). https://doi.org/10.1007/978-981-32-9433-2_27
Zhou, Y.-L., Niinomi, M., Akahori, T., Nakai, M., Fukui, H.: Comparison of various properties between titanium-tantalum alloy and pure titanium for biomedical applications. Mater. Trans. **48**(3), 380–384 (2007). https://doi.org/10.2320/matertrans.48.380